CrossMark

Assessing the accuracy of NRTK altimetric positioning for precision agriculture: test results in an olive grove environment in Southeast Spain

M. S. Garrido[1,2] · M. C. de Lacy[1,2] · M. I. Ramos[1,2] · M. J. Borque[1,2] · M. Susi[2]

Abstract

Soil erosion modeling in olive groves requires precise and accurate spatial data for the representation of topography associated with each time epoch considered. The precision and accuracy of altimetric values affect the quality of the digital elevation model (DEM) and therefore these requirements must be added to the necessity to generate high resolution DEMs. The increase of quality implies: 1. Improving the quality of the instrumentation and methodology applied in the field data collection and 2. Minimizing errors from the interpolation algorithm used to generate the digital terrain model. Currently, RTK networks are an indispensable complement to global navigation satellite systems (GNSS) precise positioning. The availability of highly accurate three-dimensional real time positioning has opened the door to new applications, making network-based real time kinematic (NRTK) positioning an attractive spatial data source for modeling soil erosion in small areas. This paper analyzes the quality of NRTK altimetric positioning supported by a local active network and its application in a test olive grove in SE Spain for soil erosion modeling. An evaluation procedure was implemented at several test sites distributed throughout an olive grove environment with special emphasis on filtering and checking the NRTK solutions in the vertical component. The precision in this component revealed a mean value of 15 mm and the vertical accuracy reached maximum values of 30 mm. In order to generate high resolution and accuracy DEM from the NRTK data, cross sections on the test olive grove were surveyed. The average altimetric quality value (CQ1D) of points surveyed was 0.017 m, according to the standard deviation estimated at test points. Based on the quality results, NRTK positioning is an accurate and reliable methodology for monitoring the erosion processes of small areas in an olive grove environment.

✉ M. S. Garrido
mgarrido@ujaen.es

1   Center for Advanced Studies in Earth Sciences, University of Jaén, Las Lagunillas Campus, 23071 Jaén, Spain

2   Department of Cartographic, Geodetic and Photogrammetric Engineering, University of Jaén, Las Lagunillas Campus, 23071 Jaén, Spain

Introduction

Accurate DEMs on soil erosion modelling

Erosion has been recognized as one of the most significant environmental problems world-wide, and its effects on the environment should not be ignored (Bakker et al. 2007). Specifically, soil erosion in olive orchards in the southeast of the Iberian Peninsula is one of the major threats to the sustainability of this crop (Gómez et al. 2014). Soil erosion is a problem that produces an important impact on the landscape, especially in olive areas. Multiple factors interact in the erosion processes in olive groves, highlighting the characteristics of the soil and the terrain topography. It is necessary to use precise spatial data in order to better quantify the changes that take place as a result of meteorological factors, properties of the land, tillage practices or slope of the terrain.

In the south of Spain, in the Andalusian Community, intensive olive farming is a major cause of soil erosion, especially on slopes. The province of Jaén, in the SE of Andalusia, has over 550,000 ha of olive groves, representing approximately 23% of the Spanish surface and 38% of the Andalusian. Almost half of the agricultural area of the province of Jaén is under cultivation with olive groves according to data from the Survey on Cultivation Areas and Crop Yields in Spain, ESYRCE (Spanish Ministry of Agriculture, Food and Environment 2013). This province is the world's largest producer of olive oil, so consideration of this industry as a "strategic sector" of the province is unquestionable given its contribution to the economy and local employment and also its environmental, social and cultural impact.

Soil erosion modeling requires precise and accurate spatial data for the representation of topography associated with each time epoch considered (Ramos et al. 2008). The model obtained must be as precise as the amount of erosion that is to be detected in the shortest time. In these studies, high resolution digital elevation models (DEMs) are essential, since the use of a lower resolution may result in substantial loss of detail (Hancock 2005). High resolution DEMs are required so that the products derived from them have an adequate level of detail. The accuracy of the digital elevation models that reflect the changes produced in the eroded terrain is a fundamental factor. The accuracy of elevations or altitude values affect the quality of DEMs, so this requirement must be added to the necessity to generate high resolution DEMs (Ramos et al. 2011).

At present, DEMs are increasingly used to generate models capable of accurately representing the surface under study. The increase of DEM quality implies: 1. Improving quality of the instrumentation and methodology applied in field data collection, and 2. Minimizing errors from the interpolation algorithm used to generate the terrain model. Detailed three-dimensional information on the land surface can currently be obtained in order to produce digital elevation models (Lucieer et al. 2014). As shown in Liu et al. (2011), DEM accuracy is very sensitive to horizontal resolution, vertical precision and the density of sample points as well as the source of the elevation data.

At present, there are several techniques and methodologies used to capture spatial information. For monitoring soil erosion, the methodologies usually employed are classical topographic surveys using total station measurements, photogrammetric techniques and remote data acquisition. Technologies such as Light Detection And Ranging (LIDAR) sensors which have been integrated with Unmanned Aerial System (UAS) (Colomina and Molina 2014), facilitate the analysis of spatial variability by allowing three-dimensional survey data to be collected both rapidly and at high spatial density where vegetation is not

present (Harley et al. 2011). Geodetic positioning methods are also being widely used in this field due to advances in technology, computing and telecommunications.

Real time positioning: applications in precision agriculture

Space geodesy, based on the determination of the three-dimensional position on the earth's surface from observations by artificial satellites, allows the determination of 3D positions in real time with centimetric accuracy. The most commonly used positioning method is real time kinematic (RTK) positioning. The main limitation of traditional RTK positioning is caused by distance-dependent errors such as orbital errors and ionospheric and tropospheric refraction, being limited to 10 km in order to resolve the ambiguities of the carrier phase (Wanninger 2008). However, these errors can be modeled using observations from several reference stations around the user position, extending the RTK positioning from one single reference station (SRS) to a multiple reference station solution or network solution (NRTK) (Takac and Zelzer 2008). At present RTK networks, known as active networks, are an indispensable complement to positioning systems. The availability of highly accurate three-dimensional real time positioning has opened the door to new applications. Some examples of applications are the use in precision agriculture (Freeland et al. 2012; Ortiz et al. 2013) and monitoring the evolution of dune systems (Garrido et al. 2013), among other innovative applications related to environmental disciplines that make use of geospatial information in real time. With real time kinematic positioning based on active networks, high accuracy in the vertical component can be obtained under optimal conditions. RTK positioning is a fast and cost-effective method for collecting topographic data, making NRTK positioning an attractive spatial data source for modeling soil erosion. However, in this field of research, it is very important to know the quality of NRTK altimetric positioning, namely the service coverage, the precision and accuracy of vertical positioning, the phase ambiguities resolution time or the repeatability and stability of the NRTK solution. In the last decade there have been studies evaluating the quality of RTK positioning. These include those conducted by Gumus et al. (2016) in Turkey, Giménez et al. (2011) in Spain and Edwards et al. (2010) in the UK to name a few. Most of these studies focused their interest on the positional quality of the RTK solutions, regardless of the characteristics of the research environment. However, it is essential to check and evaluate the performance and accuracy of precise positioning provided by an active network in an environment of olive groves in order for it to be applied in erosion studies. Crop type may influence the use of NRTK positioning due to the reduced reliability caused by the availability of few satellites, the presence of errors such as multipath and communications problems in receiving NRTK corrections. Applications of real-time GNSS positioning in precision agriculture include topographic mapping, exploration crop yield maps and guided machinery. Many examples are found in Pérez-Ruiz et al. (2015, 2011), Farooque et al. (2013) and Fountas et al. (2011). Nevertheless, references regarding the evaluation of real-time GNSS positioning in an olive grove environment are scarce and, in general, accuracy statistics have not been reported.

   The focus of this paper is to analyze the quality of NRTK altimetric positioning in order to generate high resolution and accurate DEMs for soil erosion modeling in a test olive grove. For this purpose, the precision and accuracy of NRTK altimetric positioning offered by the Andalusian Positioning Network (RAP) in the province of Jaén (SE Spain) were evaluated. This is based on the application of a testing procedure at different scenarios in an olive grove environment distributed throughout the province. The first scenario considered

a set of test sites distributed over the region in which to apply a specially designed NRTK test and the second one a test olive grove surveyed considering the RAP NRTK solution previously analyzed.

High accuracy positioning services in Andalusia from RAP network

The Andalusian Positioning Network (RAP) is a local geodetic infrastructure for precise positioning applications in the Andalusian Community (S Spain), managed by the Institute of Statistics and Cartography of Andalusia (IECA) (Páez et al. 2017). The RAP network provides both GNSS observations and differential NRTK corrections for accurate positioning in precision agriculture, machine guidance and many other geomatic applications in the community of Andalusia. As Garrido et al. (2018) show, RAP generates network corrections using the Master-Auxiliary Concept (MAC) introduced by Euler et al. (2001). This approach was designed to transmit NRTK corrections in standard RTCM format to the user in a compact form (Euler and Zebhauser 2003), representing ambiguity-levelled observation data as correction differences of dispersive (ionospheric delay) and non-dispersive data (tropospheric delay and orbit errors) for each satellite-receiver pair (Janssen 2009). Leica SpiderNet software processes the observations of RAP reference stations around the user and produces NRTK corrections that are broadcast to the users under the Networked Transport of RTCM via Internet Protocol (NTRIP).

Materials and methods

Scenario 1: test sites

In order to explore the performance of NRTK positioning assisted by the RAP network for precision agriculture studies in an olive grove environment, GNSS measurements were carried out at test sites to determine: the time to fix ambiguities in real time (time from receiving the first correction data from the control center until a fixed solution of the rover is achieved), the precision, the accuracy and the repeatability of NRTK solutions.

The test sites selected were geodetic sites belonging to the REGENTE network, a Spanish 3D National Geodetic Network surveyed by the Spanish National Geographic Institute (IGNE). Each REGENTE geodetic site is comprised of a cylinder 1.20 m in height and 0.30 m in diameter supported on a concrete base, with a reinforced center to ensure an accurate and stable placement. For this study, seven REGENTE sites were selected in the province of Jaén (SE Spain) on the basis of information available in the IGNE's geographical databases. One additional test site ("OLIV") expressly built at the test olive grove is a concrete pillar anchored to the ground that incorporates an embedded reinforced centering system (Fig. 1). Their distribution in the region (Fig. 2) is in accordance with the objectives of this study, which are to represent sites in an olive grove environment, inside the active network, at moderate distance from the nearest reference station and with a wide range of average elevation differences to the surrounding RAP reference stations.

At each test site, the instruments used included two GNSS receivers, model GS10, (Equipment Numbers 3660835 and 3660839) connected to the same GNSS antenna AS10 (Leica Geosystems AG. Heerbrugg, Switzerland) (Fig. 1). The first GNSS receiver was equipped with a Siemens MC75 GSM/GPRS module and configured to receive MAC
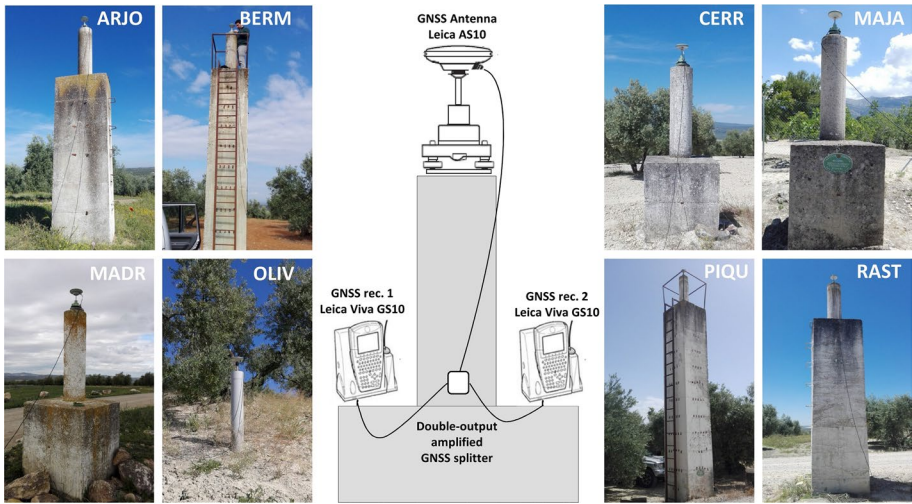
Fig. 1 GNSS instrumentation applied at test sites selected in an olive grove environment (Southeast Spain)
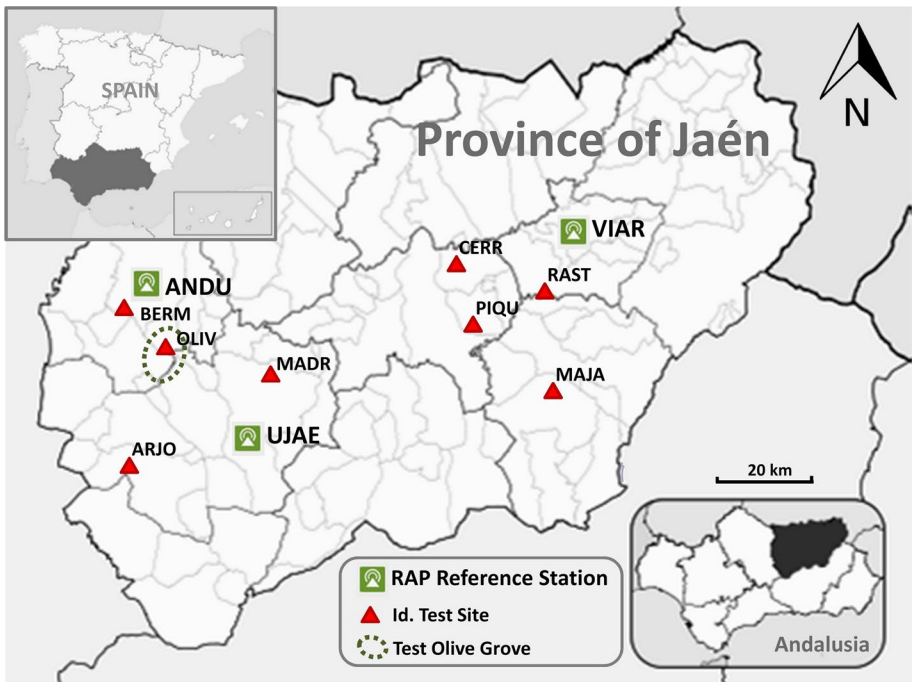

Fig. 2 Distribution of RAP reference stations and test sites and location of the test olive grove in the province of Jaén (Andalusia-Southeast Spain)

NRTK corrections through the RAP NTRIP server. Each NRTK solution was stored only if the horizontal and vertical co-ordinate quality (CQ2D and CQ1D) was below 30 and 50 mm respectively. The co-ordinate quality (CQ) was computed on the rover for code

solutions and phase fixed solutions. This is an indicator of the quality of the observations, the current satellite constellation and the different environmental conditions, and is derived so that there is at least a two-third probability that the computed position deviates from the true position by less than the CQ value. It is important to underline the fact that CQ is different from the standard deviation. The standard deviation as CQ would often be too optimistic, therefore the computation of the CQ is not based on the basic standard deviation algorithms. There is a 39.3% statistical probability in 2D (a 68.3% statistical probability in 1D) that the computed position deviates from the true position by less than the standard deviation. This probability is not enough for a reliable quality indicator. This unreliability is particularly true for low redundancy situations such as a constellation of four satellites. In such a case, the RMS converges to zero and the standard deviation would show an unrealistically small value (Leica Geosystems 2014).

With this equipment configuration, RTK tests were applied at test sites for three sessions per day (Session 1: morning; Session 2: mid-day and Session 3: afternoon). Every successive measurement session is carried out in the time interval of minimally 90 min because this allows the elimination of the influences resulting from the changes of satellite configuration and ionosphere variations. Each test had a sample size of 90 positions, 30 per session. In order to reduce the correlation between different NRTK solutions and to guarantee the independence between different ambiguities resolutions, after recording each NRTK position, the GNSS receiver was disconnected from the RAP NTRIP caster and not connected again until the phase solution was lost. The maximum time required to solve integer ambiguities in real-time after re-initialization is fixed at 60 s. A second GNSS receiver was connected simultaneously to the same AS10 antenna via a double-output amplified source splitter to record 6 h of GNSS data with an observation sampling rate of 30 s in order to allow the accurate determination of test site co-ordinates. The GNSS observation at each test site was post-processed relative to the three nearest RAP reference stations using Bernese 5.0 software (Dach et al. 2007). The main options used in the GPS data processing are shown in Table 1. This ensured that the control co-ordinates considered for each test site and each NRTK position were in a compatible realization of ETRS89 (ETRF05).

The co-ordinates estimated for the test sites are summarized in Table 2, including the observation date, their ETRS89 Cartesian co-ordinates (ETRS89) and the distance to the three RAP nearest reference stations considered. Finally, the NRTK measurements were validated with the post-processed solutions at test sites. That is to say that the NRTK positions collected at each test site were used to determine the differences between the 'control' value (co-ordinates estimated by adjusted post-processing solution) and each NRTK position. These differences are expressed in a local reference system as Easting (E), Northing (N) and Up (U) components (Ghilani and Wolf 2010).

Scenario 2: test olive grove

The test olive grove is also located in the province of Jaen (Andalusia) (Fig. 2) and it was chosen for being representative of the majority of the olive plots in the South of Spain. The olive orchard is 1.2 ha with 120 olive trees of similar characteristics. They all have three trunks, are about 35 years old, with a medium olive crown diameter around 5 m and their mean fruit harvest is 60 kg per year. The test olive orchard is unirrigated where the slope gradient varies between 2 and 25%. In this test olive grove, sediment transport is very significant due to "tillage erosion", which is considered a form of erosion that moves soil

Table 1 Characteristics of GPS processing with BERNESE 5.0 software

Pre-processing	Pre-processing in a baseline by baseline mode using triple-differences for cycle correction
Basic observable	Carrier phase (code only used for receiver clock synchronization) Elevation angle cut-off: 3 degrees + elevation dependent weighting
Modeled observable	Double-differences, ionosphere-free linear combination
Data sampling	30 s
Earth Geopotential model	JGM3
Ocean loading model	FES2004 (Lyard et al. 2006)
Ocean tides	OT_CSRC
Atmospheric loading	Not applied
Solid Earth tides	Applied (IERS Conventions 96/2000)
Orbits and ERPs	IGS final orbit and ERP information (Dow et al. 2005)
Planetary ephemeris	DE200 from JPL
Ground and satellite antennae center calibration	Absolute antenna phase centre corrections based on IGS08 model
Troposphere	Dry-Niell as a priori model, estimation of zenith delay corrections at 1-h intervals for each station using the wet-Niell Mapping Function (Niell 1996). Troposphere zenith path delay is modeled as a piece-wise linear (i.e., continuous) function. Horizontal gradient parameters are not estimated
Adjustment	Weighted least-squares algorithm with correct correlations
Datum definition	From the ETRF05 co-ordinates of the three closest reference stations constrained to 2 mm in the north and east components and 4 mm in the vertical component
Ambiguity	QIF strategy to resolve ambiguities for each baseline. Resolved ambiguities introduced into final solution
Satelliteclock	Satellite clock biases are not estimated but bias eliminated by forming double-differences
Receiver clock	Receiver clock corrections are estimated during the bias pre-processing using code measurements

Table 2 Test sites selected, including observation date, ETRS89 cartesian co-ordinates (post-processed adjusted solution) and baseline length (D) to the three RAP reference stations considered for post-processing solution (the baseline for the nearest station –master station- is shown in bold type)

Test site	Observation	Post-processed solution (ETRS89)			Baseline length		
Id.	DOY/Year	X (m)	Y (m)	Z (m)	D_{ANDU} (m)	D_{UJAE} (m)	D_{VIAR} (m)
ARJO	117/2016	5,038,513.9381	− 357,940.1662	3,882,213.7742	34,475.949	**25,621.848**	104,333.155
BERM	113/2016	5,018,989.2222	− 357,663.2379	3,906,965.0752	**4927.411**	36,129.762	94,845.062
CERR	154/2016	5,017,145.6861	− 289,525.2465	3,915,232.5129	64,285.986	55,102.192	**26,295.945**
MADR	111/2016	5,029,488.0244	− 328,001.7500	3,896,353.0431	30,981.643	**12,447.030**	70,116.947
MAJA	152/2016	5,034,199.7963	− 269,659.1184	3,895,279.8460	86,635.978	63,792.399	**32,496.131**
OLIV	148/2016	5,023,926.4971	− 349,680.1577	3,901,346.3109	**10,841.969**	25,220.948	88,398.136
PIQU	181/2016	5,024,879.7239	− 285,701.4883	3,905,835.1361	68,306.370	52,026.312	**28,241.766**
RAST	153/2016	5,021,388.6611	− 270,454.0644	3,911,219.6067	83,186.898	68,560.386	**13,271.872**

from the top of the field downward. Consequently, in this study, the main component to be considered is the altimetric component.

In order to analyze this movement accurately, the measurement technique applied considers a set of cross sections or altimetric profile lines established on the test olive grove. The altimetric profiles surveyed in this study are oriented mostly Northeast-Southwest with an approximate azimuth of 11 degrees according to the maximum slope. The distance between adjacent profiles is 1.5 m and this distance is maintained between consecutive points in the same profile. Thirty three cross sections with a mean length of 280 m were established on the test olive grove (Fig. 3). Each point was surveyed considering the MAC NRTK solution from the RAP network. When a point is surveyed within a profile, the maximum distance considered perpendicular to the reference line is 0.100 m. This tolerance is established as $3.5\sigma_P = \pm 0.100$ m (coverage probability of 99.7%) where σ_P is standard uncertainty in the 2D position fixed at 0.030 m coincident with the CQ2D.

The reference observation campaign was undertaken in June, 2016. In subsequent observation campaigns, profiles will be surveyed so that the start and end points of each are coincident with the first campaign. Although a concrete pillar is available on the test olive grove (OLIV test site), it should be noted that the framework is established by the RAP active network, avoiding the placement of a local control network in the test area. The instrumentation applied is the same one described in the previous section, a GNSS receiver GS10 and antenna AS10, but taking into account, as an additional accessory, a telescopic carbon survey pole (locks at 2.00 m) with a circular bubble and tilting platform coupled at the end of the pole (Fig. 3).

Finally, in order to generate the high resolution and accuracy DEM, an interpolation process was applied to points surveyed. Interpolation, also known as gridding, is the process of estimating unknown values of an array of cells from a set of known point observations (NRTK planimetric and altimetric positions) by applying a mathematical algorithm. Interpolation is used to generate a continuous modeling of the surface and to predict what a value would be for any given cell location covered by the raster from a limited set of input sample observations. Different interpolation methods are available: distance, inverse
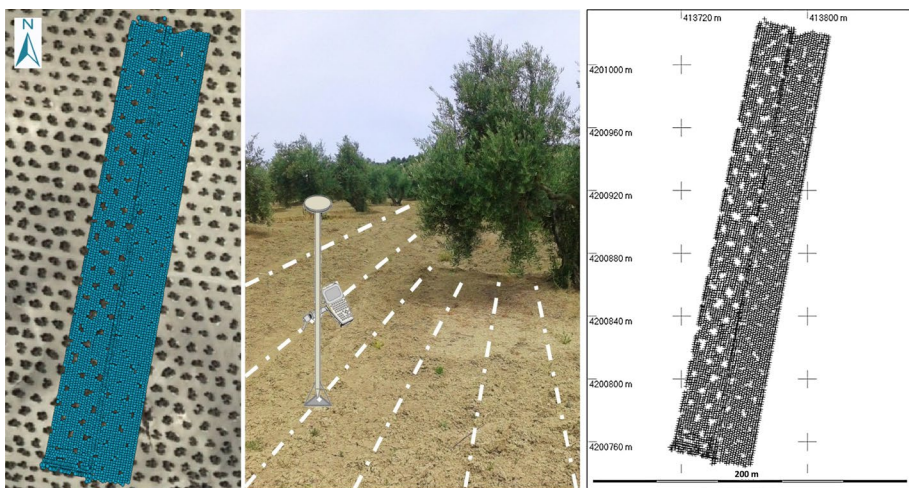
Fig. 3 Orthoimage (PNOA – IGNE) with points surveyed, detail of RTK survey procedure in the test olive grove and plane UTM grid co-ordinates for points surveyed (ETRS89/UTM Zone: 30)

distance weighting, stamping, triangulation, etc. (Guo et al. 2010). These are implemented in image-based 3D modeling and GIS software. In this application, the algorithm used to generate the DEM with MapInfo Pro Advanced V.16 is that of triangulation. The triangulation method is most suited to data that is evenly distributed over the area of interest. This method produces a regular gridded raster from a set of input data points by creating a Delaunay triangulation of the input points, from which the value at the raster cell centers is estimated by linear interpolation of the plane defined by the three nodes of the overlapping triangle. The Delaunay triangulation seeks to maximize the minimum angle in each of the triangles and will generate a mesh that entirely encompasses the convex hull of the input points.

Results and analysis

In erosion studies, the main component to be considered is the altimetric component. Thus this section provides numerical and graphical results of altimetric NRTK positioning at test sites based on the RAP network, a summary of the quality of altimetric profiles surveyed in the test olive grove considering the RAP NRTK solution and a high resolution DEM generated for the test olive grove.

NRTK altimetric solutions at test sites

An active network provides a reference frame, offering a datum-consistent solution to users of RTK services for accurate applications. The way to assess the accuracy of NRTK solutions achieved at each test site is to compare these real time results with a known reference value with a high level of accuracy (control value). Considering the technical specifications for Leica GS10 GNSS receivers, the accuracy (RMS) with Network Real-Time-Kinematic (NRTK) for horizontal and vertical positioning are respectively 8 mm + 0.5 ppm (RMS) and 15 mm + 0.5 ppm (RMS) (Standard of Compliance with ISO17123-8: "GNSS field measurement systems in real time kinematic (RTK)"—ISO 2015). On the other hand, the accuracies (RMS) for post processing (phase observations) with long sessions are 3 mm + 0.1 ppm (RMS) and 3.5 mm + 0.4 ppm (RMS) for horizontal and vertical positioning. These values can be improved if three baselines are considered and a solution from a least squares adjustment is used to determine the control co-ordinates of the test sites. If the accuracy of the NRTK vertical solution under test and the uncertainty of the post processing solution are compared, the ratio is around 4:1.

A crucial aspect in spatial data analysis is to identify and, if necessary, to remove the outliers. An outlier is defined as a data which stands far away from the other records. It is numerically distant from the rest of the data. The boxplot is a quick way of examining sets of data graphically. The boxplot uses the median and the lower and upper quartiles. The lower quartile is Q1 and the upper quartile is Q3. The difference between Q3 and Q1 is called the interquartile range. Using a boxplot, an outlier is considered as a data that is located outside the fences of the boxplot (e.g.: outside 1.5 times the interquartile range). These diagrams allow the data available for a given variable to be analyzed, in this case the NRTK Up component throughout the different observation sessions. In each diagram, it is possible to identify the outliers and to analyze visually aspects such as the symmetry, centrality or dispersion of the data. In Fig. 4, boxplots for the NRTK Up component by session at all test sites are shown. Once all records identified as possible outliers have been
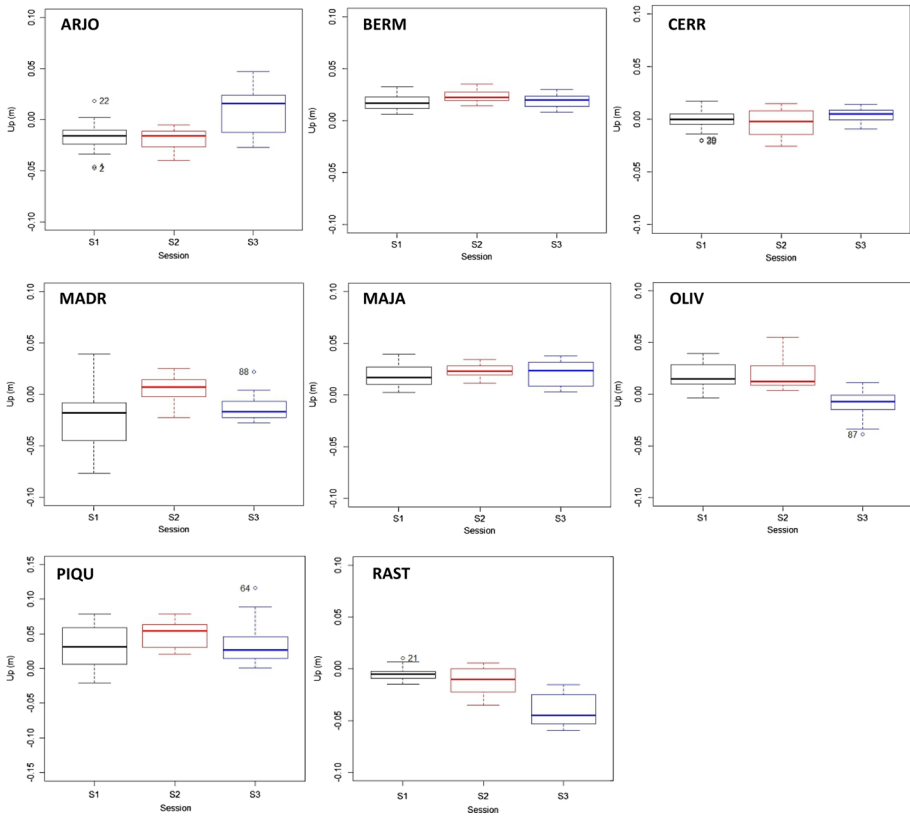
Fig. 4 Identification of potential outliers in NRTK solutions (Up component) by session at test sites

reviewed, it can be concluded that only a record of the third observation session at "PIQU" test site can be considered as an outlier and therefore must be eliminated. It should be noted that the vertical scale at the PIQU test site has been extended with respect to other test sites. The remaining values identified at the boxplots are below the limits established in the altimetric co-ordinate quality (CQ1D $\leq$ 0.050 m), therefore they are not considered as anomalous values. The test site whose NRTK altimetric solutions show a more homogeneous and less dispersion behavior is "BERM", due to the reduced distance to the nearest reference station (master station).

NRTK positioning accuracy depends mainly on the reference frame, but is also affected by the length of the baselines and the elevation difference between the reference stations and the rover position (test site). The vertical accuracy by session is computed as the mean of absolute values for the NRTK Up component. The precision in the NRTK Up component is determined by the standard deviation, a statistical value generally used to quantify the dispersion of the RTK data set. Table 3 summarizes by sessions, the sample size, the standard deviation of the NRTK Up component and the vertical accuracy at test sites selected.

Comparing the precision values shown in Table 3, the precision in the Up component is in general better than 0.030 m. The worst results are related to the first session at the PIQU test site (0.029 m). Reviewing the results presented, the vertical accuracy reaches maximum values

Table 3 Sample size (n), precision in the NRTK Up component (σ_{Up}) and vertical accuracy (V) by sessions at test sites selected considering the RAP NRTK solution

Test site	Session 1			Session 2			Session 3		
Id.	n	σ_{Up} (m)	V (m)	n	σ_{Up} (m)	V (m)	n	σ_{Up} (m)	V (m)
ARJO	30	0.013	0.019	26	0.010	0.018	30	0.021	0.020
BERM	30	0.007	0.018	30	0.006	0.023	30	0.006	0.019
CERRO	30	0.009	0.007	30	0.012	0.011	30	0.006	0.006
MADR	30	0.028	0.028	30	0.012	0.011	30	0.011	0.015
MAJA	30	0.011	0.019	30	0.006	0.023	30	0.011	0.020
OLIV	30	0.013	0.018	30	0.014	0.019	30	0.013	0.012
PIQU	30	0.029	0.034	30	0.018	0.049	29	0.024	0.033
RAST	30	0.006	0.007	30	0.013	0.013	30	0.014	0.042

around 0.030 m, except for the PIQU test site, where the worst results were recorded throughout the three observation sessions once the outlier had been eliminated. This is probably due to the NRTK accuracy being affected by the subset of reference stations considered, although the approximate position of the test site sent to the RAP control center is always the same. Changes in satellite configuration, a low number of satellites and high VDOP (Vertical Dilution of Precision) may be other possible causes. It should also be considered that the results presented in Table 3 are the average of multiple NRTK records, so a detailed analysis of each observation session is required. In order to visualize the variation in the altimetric component of each NRTK position, all observation sessions at all test sites are plotted in Fig. 5. The mean value of the NRTK Up component for each session is also represented by a continuous line.

High resolution and accuracy DEM

After the quality parameters of NRTK altimetric positioning had been tested at test sites, cross sections on the test olive grove were surveyed considering the RAP NRTK solution. There were almost 6000 points surveyed with altimetric quality values ranging from 0.007 to 0.066 m. The average value of CQ1D was 0.017 m, according to the standard deviation shown in Table 3 for the average of multiple records. Figure 6 shows the histograms generated with the altimetric (CQ1D) and the planimetric (CQ2D) quality values. As expected, it shows generally better results for the horizontal component than for the vertical component. These values are duplicated for CQ1D with respect to CQ2D. Nevertheless, as can be seen, in the subrange of values below 0.025 m is where 87.5% of the CQ1D values are concentrated. Thus, the high quality of altimetric NRTK solutions at this olive grove environment is a proven fact.

Based on the quality results, the high resolution and accuracy digital elevation model generated from the NRTK data (Fig. 7) can be considered suitable for estimating the erosion processes at this test olive grove in future studies.

Conclusions

Today, real time GNSS positioning is an important tool for different applications in precision agriculture. The use of global navigation satellite systems together with the availability of active positioning networks (NRTK positioning) is an optimal and cost-effective
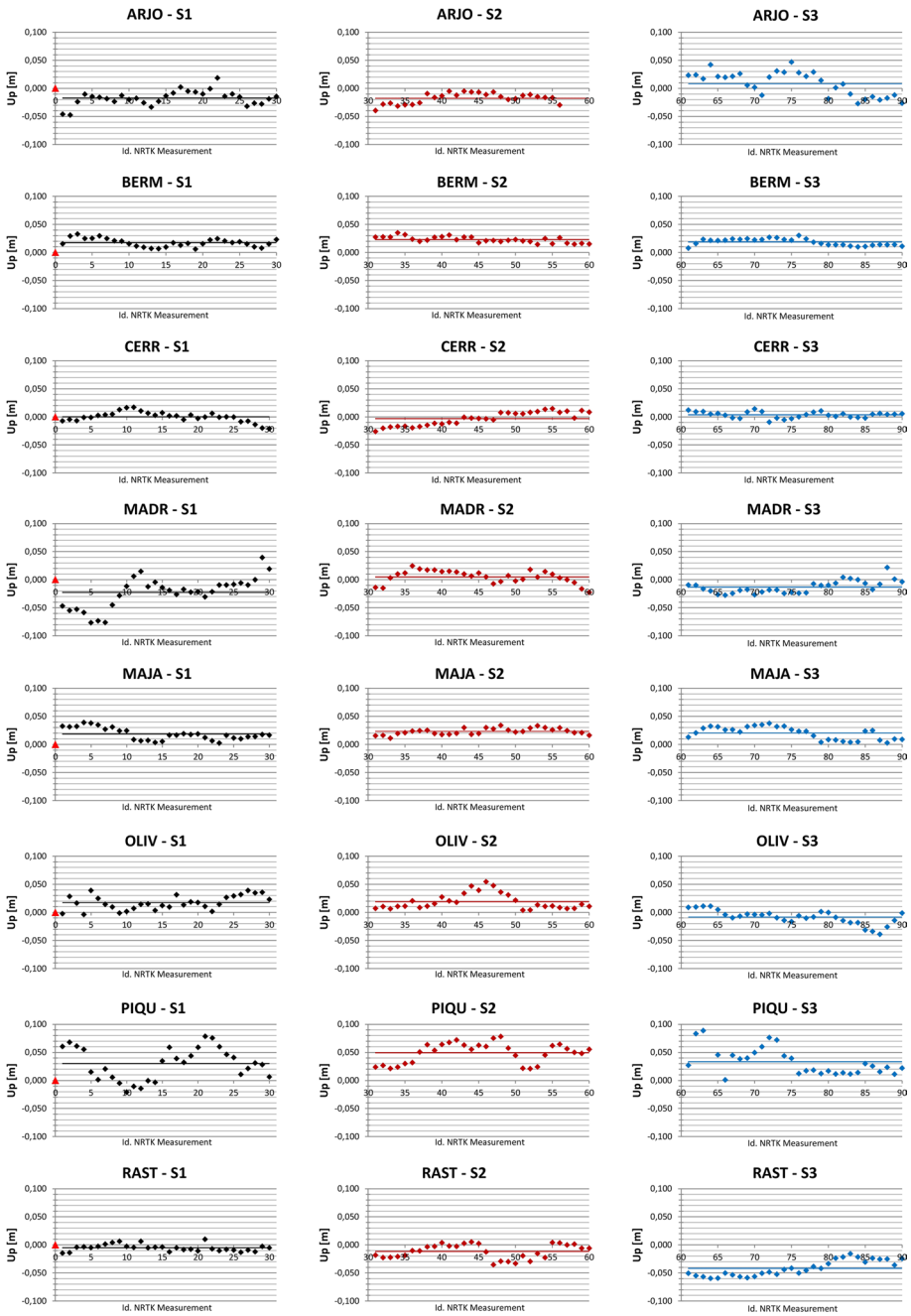
Fig. 5 Graphical results of altimetric NRTK positioning by session at test sites based on the RAP network (reference value: adjusted post-processing solution)
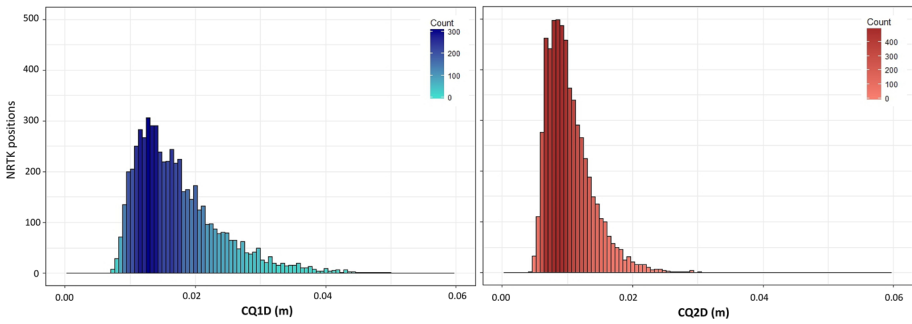
Fig. 6 Histograms with altimetric quality values -CQ1D- (left) and planimetric quality values -CQ2D- (right) for points surveyed at the test olive grove considering the RAP NRTK solution
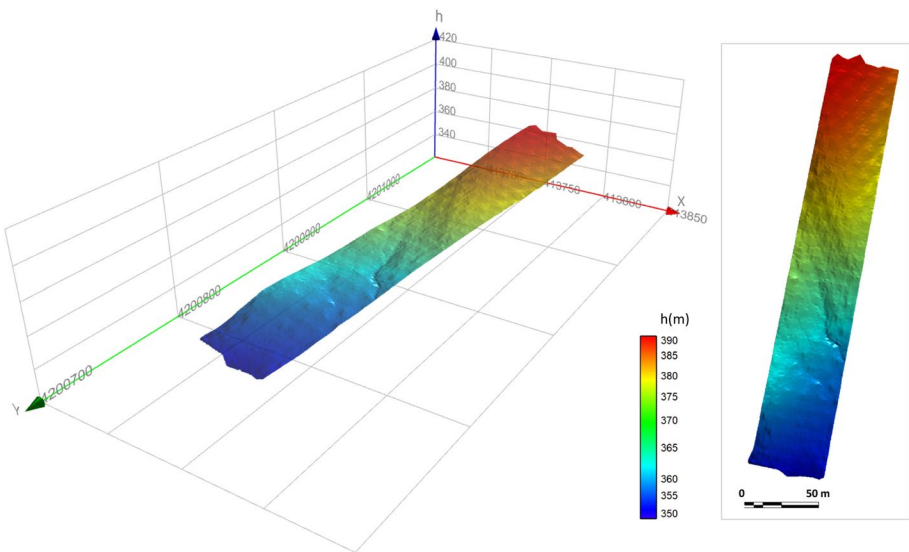
Fig. 7 High resolution DEM and plan view of the test olive grove (ETRS89/UTM Zone: 30/Ellipsoidal altitude). Reference epoch: June 2016

option to be applied in studies of erosion processes. However, it is important to ensure the accuracy achieved using this methodology, especially in the altimetric component. It is very important to know how precise and accurate the spatial data are so that the reliability and the validity of the results derived from them can best be considered.

The main objective of this study was to apply an accuracy assessment methodology for NRTK positioning supported by a local active network, with special emphasis on filtering and checking the altimetric data obtained. Focusing on this aspect, a RTK test was applied in order to check the quality of real time altimetric positioning based on the RAP network at eight test sites located in an olive grove environment. The graphical and numerical results show that the MAC real time network solution offers high precision and vertical accuracy together with a homogeneous and stable behavior in the environment where the test has been applied. NRTK solutions introduce significant improvements in vertical positioning such as high repeatability, accuracy and reliability, being an accurate and reliable

technique for monitoring soil erosion in small areas. The NRTK solution in altimetric positioning has been applied to survey elevation profiles in a test olive grove for the generation of a high resolution and precision digital elevation model. The DEM generated with this technique will be applied in the study of erosion processes in this olive grove environment. In order to detect changes in olive grove terrain morphology, detailed spatial information can be obtained by repeated GNSS surveys and an active network guarantees the reference frame for different observations campaigns.

Through the use of network RTK solutions and high accurate DEMs, precision agriculture will enable the impact of tillage erosion in the olive grove environment to be shown and the relevant agricultural practices to be adapted. NRTK solutions achieve high reliability, showing the great potential that this technique offers to the agricultural sector.

References

Bakker, M. M., Govers, G., Jones, R. A., & Rounsevell, M. D. A. (2007). The effect of soil erosion on Europe's crop yields. *Ecosystems, 10,* 1209–1219. https://doi.org/10.1007/s10021-007-9090-3.

Colomina, I., & Molina, P. (2014). Unmanned aerial systems for photogrammetry and remote sensing: A review. *ISPRS Journal of Photogrammetry and Remote Sensing, 92,* 79–97. https://doi.org/10.1016/j.isprsjprs.2014.02.013.

Dach, R., Hugentobler, U., Fridez, P., Meindl, M. (2007). Bernese GPS software version 5.0 user manual. Astronomical Institute, University of Bern, Switzerland, 612 pp. Retrieved from http://www.bernese.unibe.ch/docs50/DOCU50.pdf. Accessed July 5, 2018.

Dow, J. M., Neilan, R. E., & Gendt, G. (2005). The International GPS Service: celebrating the 10th anniversary and looking to the next decade. *Advances in Space Research, 36*(3), 320–326. https://doi.org/10.1016/j.asr.2005.05.125.

Edwards, S. J., Clarke, P. J., Penna, P. N., & Goebell, S. (2010). An examination of network RTK GPS services in Great Britain. *Survey Review, 42*(316), 107–121. https://doi.org/10.1179/003962610X12572516251529.

Euler, H.-J., Keenan, C. R., Zebhauser, B. E., & Wübbena, G. (2001). Study of a simplified approach in utilizing information from permanent reference station arrays. *In Proceedings of ION GPS 2001* (pp. 379–391). Manassas, VA, USA: Institute of Navigation.

Euler, H. J., & Zebhauser, B. E. (2003). The use of standardized network RTK messages in rover applications for surveying. In *Proceedings of the 2003 National Technical Meeting of the Institute of Navigation* (pp. 377–384). Manassas, VA, USA: Institute of Navigation.

Farooque, A. A., Chang, Y. K., Zaman, Q. U., Groulx, D., Schumann, A. W., & Esau, T. J. (2013). Performance evaluation of multiple ground based sensors mounted on a commercial wild blueberry harvester to sense plant height, fruit yield and topographic features in real-time. *Computers and Electronics in Agriculture, 91,* 135–144. https://doi.org/10.1016/j.compag.2012.12.006.

Fountas, S., Aggelopoulou, K., Bouloulis, C., Nanos, G. D., Wulfsohn, D. Gemtos, et al. (2011). Site-specific management in an olive tree plantation. *Precision Agriculture, 12,* 179–195. https://doi.org/10.1007/s11119-010-9167-4.

Freeland, R. S., Buschermohle, M. J., Wilkerson, J. B., & Pierce, J. C. (2012). Precision agriculture-assessing virtual and single reference stations. *Applied Engineering in Agriculture, 28*(6), 913–922. https://doi.org/10.13031/2013.42466.

Garrido, M. S., de Lacy, M. C., & Rojas, A. M. (2018). Impact of tropospheric modelling on GNSS vertical precision: An empirical analysis based on a local active network. *International Journal of Digital Earth, 11*(9), 880–896. https://doi.org/10.1080/17538947.2017.1367040.

Garrido, M. S., Giménez, E., Ramos, M. I., & Gil, A. J. (2013). A high spatio-temporal methodology for monitoring dunes morphology based on precise GPS-NRTK profiles: Test-case of Dune of Mónsul

on the south-east Spanish coastline. *Aeolian Research, 8,* 75–84. https://doi.org/10.1016/j.aeoli a.2012.10.011.

Ghilani, C. D., & Wolf, P. R. (2010). *Adjustment computations: Spatial data analysis*. Hoboken, NJ, USA: Wiley. https://doi.org/10.1002/9780470586266.

Giménez, E., Garrido, M. S., De Lacy, M. C., & Gil, A. J. (2011). Comparing RTK positioning from updated REGAM and MERISTEMUM CORS networks in Southeast Spain. *Journal of Applied Geodesy, 5,* 23–35. https://doi.org/10.1515/jag.2011.003.

Gómez, J. A., Infante-Amate, J., de González Molina, M., Vanwalleghem, T., Taguas, E., & y Lorite, I. (2014). Review: Olive cultivation, its impact on soil erosion and its progression into yield impacts in Southern Spain in the past as a key to a future of increasing climate uncertainty. *Agriculture, 4,* 170–198. https://doi.org/10.3390/agriculture4020170.

Gumus, K., Selbesoglu, M. O., & Celik, C. T. (2016). Accuracy investigation of height obtained from Classical and Network RTK with ANOVA test. *Measurement, 90,* 135–143. https://doi.org/10.1016/j.measurement.2016.04.045.

Guo, Q., Li, W., Yu, H., & Alvarez, O. (2010). Effects of topographic variability and lidar sampling density on several DEM interpolation methods. *Photogrammetric Engineering & Remote Sensing, 76*(6), 701–712. https://doi.org/10.14358/PERS.76.6.701.

Hancock, G. R. (2005). The use of digital elevation models in the identification and characterization of catchments over different grid scales. *Hydrological Processes, 19,* 1727–1749. https://doi.org/10.1002/hyp.5632.

Harley, M. D., Turner, I. L., Short, A. D., & Ranasinghe, R. (2011). Assessment and integration of conventional, RTK-GPS and image-derived beach survey methods for daily to decadal coastal monitoring. *Coastal Engineering, 58*(7–8), 194–205. https://doi.org/10.1016/j.coastaleng.2010.09.006.

ISO. (2015). *ISO 17123-8:2015—optics and optical instruments—field procedures for testing geodetic and surveying instruments—Part 8: GNSS field measurement systems in real-time kinematic (RTK).* Geneva, Switzerland: ISO.

Janssen, V. (2009). A comparison of the VRS and MAC principles for network RTK. In *Proceedings of IGNSS Symposium* (pp. 1–13). NSW, Australia: IGNSS Society Inc.

Leica Geosystems. (2014). *Leica viva series technical reference manual*. Heerbrugg, Switzerland: Leica Geosystems AG.

Liu, H., Kiesel, J., Hörmann, G., & Fohrer, N. (2011). Effects of DEM horizontal resolution and methods on calculating the slope length factor in gently rolling landscapes. *CATENA, 87,* 368–375. https://doi.org/10.1016/j.catena.2011.07.003.

Lucieer, A., De Jong, S. M., & Turner, D. (2014). Mapping landslide displacements using Structure from Motion (SfM) and image correlation of multi-temporal UAV photography. *Progress in Physical Geography, 38*(1), 97–116. https://doi.org/10.1177/0309133313515293.

Lyard, L., Lefevre, L., Letellier, T., & Francis, O. (2006). Modelling the global ocean tides: Modern insights from FES2004. *Ocean Dynamic, 56,* 394–415. https://doi.org/10.1007/s10236-006-0086-x.

Niell, A. E. (1996). Global mapping functions for the atmosphere delay at radio wavelengths. *Journal of Geophysical Research, 101*(2), 3227–3246. https://doi.org/10.1029/95JB03048.

Ortiz, B. V., Balkcom, K. B., Duzy, L., Van Santen, E., & Hartzog, D. L. (2013). Evaluation of agronomic and economic benefits of using RTK-GPS-based auto-steer guidance systems for peanut digging operations. *Precision Agriculture, 14,* 357–375. https://doi.org/10.1007/s11119-012-9297-y.

Páez, R., Torrecillas, C., Barbero, I., & Berrocoso, M. (2017). Regional positioning services as economic and construction activity indicators: The case study of Andalusian Positioning Network (Southern Spain). *Geocarto International, 32*(1), 44–58. https://doi.org/10.1080/10106049.2015.1120358.

Pérez-Ruiz, M., Agüera, J., Gil, A. J., & Slaughter, D. C. (2011). Optimization of agrochemical application in olive groves based on positioning sensor. *Precision Agriculture, 12,* 564–575. https://doi.org/10.1007/s11119-010-9200-7.

Pérez-Ruiz, M., Gonzalez-de-Santos, P., Ribeiro, A., Fernandez-Quintanilla, C., Peruzzi, A., & Vieri, M. (2015). Highlights and preliminary results for autonomous crop protection. *Computers and Electronics in Agriculture, 110,* 150–161. https://doi.org/10.1016/j.compag.2014.11.010.

Ramos, M. I., Feito, F. R., Gil, A. J., & Cubillas, J. J. (2008). A study of spatial variability of soil loss with high resolution DEMs: a case study of a sloping olive orchard in southern Spain. *Geoderma, 148,* 1–12. https://doi.org/10.1016/j.geoderma.2008.08.015.

Ramos, M. I., García, A. L., Garrido, M. S., Feito, F. R., & Gil, A. J. (2011). Control of real time GPS data to analyze the erosion in an olive farm. In N. Mastorakis, V. Mladenov, C. M. Travieso-Gonzalez, & M. Kohler (Eds.), *Proceeding of the 2nd European Conference of Control ECC '11, Recent Researches in Engineering and Automatic Control* (pp. 19–23). WSEAS Press.

Spanish Ministry of Agriculture, Food and Environment. (2013). Survey on Cultivation Areas and Crop Yields in Spain, ESYRCE (in Spanish).

Takac, F., & Zelzer, O. (2008). The relationship between network RTK solutions MAC, VRS, PRS, FKP and i-MAX. In *Proceedings of ION GNSS 2008* (pp. 348–355). Manassas, VA, USA: Institute of Navigation.

Wanninger, L. (2008). Introduction to Network RTK. IAG Working Group 4.5.1: Network RTK (2003–2007). Retrieved from (http://www.wasoft.de/e/iagwg451/intro/introduction.html). Accessed July 5, 2018.